J|A|C|S
ARTICLES
Published on Web 06/29/2004

Two-Dimensional Crystallization: Self-Assembly, Pseudopolymorphism, and Symmetry-Independent Molecules

Katherine E. Plass, Kibum Kim, and Adam J. Matzger*

Contribution from the Department of Chemistry and the Macromolecular Science and Engineering Program, The University of Michigan, Ann Arbor, Michigan 48109-1055

Received February 5, 2004; E-mail: matzger@umich.edu

Abstract: The self-assembly of a series of 1,3-disubstituted benzenes has been scrutinized by scanning tunneling microscopy (STM) and computational modeling. Small changes in the functional groups (e.g., ester, thioester, ketone) resulted in dramatic changes in packing patterns. Remarkably, several of the molecules gave rise to monolayers with more than one molecule in the asymmetric unit and displayed multiple packing patterns. This constitutes the most complex behavior observed to date in this type of monolayer and illuminates several issues of importance in three-dimensional crystallization. Intermolecular interactions associated with the observation of multiple molecules in the asymmetric unit and stabilization of pseudopolymorphs were identified. The geometry and electrostatic properties of the isolated molecule and monolayer density were found to be critical in determining which packing motif was adopted.

Introduction

Predicting and understanding the phenomenon of crystallization is of great scientific and technological importance because crystal structure determines key solid-state properties such as the bioavailability of pharmaceutical solids and the performance of electronic materials. Unfortunately, the ability to routinely predict three-dimensional crystal structures of even the simplest molecules in common space groups remains a distant goal despite an intensive worldwide effort.[1−3] A reductionist approach to understanding crystallization is to decrease the dimensionality of the problem. One particularly promising model is the assembly of two-dimensional crystals by physisorption at the liquid−solid interface.[4−10] Complexities inherent to three-dimensional crystallization remain in this model system, including the possibility of more than one crystallographically unique molecule existing in a given crystal structure[11,12] and multiple energetically achievable packing motifs.[13−16] The latter phenomenon is termed crystalline polymorphism in three-dimensions,[17] while the former refers to structures with $Z' > 1$. In common usage, Z' describes the number of molecules in an asymmetric unit. More rigorously, it is the number of formula units in the unit cell divided by the number of independent general positions.[18] Thus, a structure with $Z' = 1$ could be composed of two inequivalent half-molecules, resulting in two different types of molecules in the structure, or one unique molecule. Although several general molecular features have been correlated with $Z' > 1$, serious scrutiny in three-dimensions has not yielded a general explanation for the frequency and conditions of occurrence (vide infra).[18−20] The factors leading to polymorphism in three-dimensions have remained equally difficult to define.[17] An important simplification in the two-dimensional crystal packing problem is that only 17 space groups are needed to describe the possible symmetry element combinations instead of the 230 required to describe packing in three-dimensions. This reduction in the number of potential packing patterns, and the smaller number of intermolecular

(1) Motherwell, W. D. S.; Ammon, H. L.; Dunitz, J. D.; Dzyabchenko, A.; Erk, P.; Gavezzotti, A.; Hofmann, D. W. M.; Leusen, F. J. J.; Lommerse, J. P. M.; Mooij, W. T. M.; Price, S. L.; Scheraga, H.; Schweizer, B.; Schmidt, M. U.; van Eijck, B. P.; Verwer, P.; Williams, D. E. *Acta Crystallogr., Sect. B: Struct. Sci.* **2002**, *58*, 647−661.
(2) Lommerse, J. P. M.; Motherwell, W. D. S.; Ammon, H. L.; Dunitz, J. D.; Gavezzotti, A.; Hofmann, D. W. M.; Leusen, F. J. J.; Mooij, W. T. M.; Price, S. L.; Schweizer, B.; Schmidt, M. U.; van Eijck, B. P.; Verwer, P.; Williams, D. E. *Acta Crystallogr., Sect. B: Struct. Sci.* **2000**, *56*, 697−714.
(3) For recent reviews of the challenges of three-dimensional crystal structure prediction, see: Desiraju, G. R. *Nat. Mater.* **2002**, *1*, 77−79. Dunitz, J. D. *Chem. Commun.* **2003**, 545−548.
(4) De Feyter, S.; De Schryver, F. C. *Chem. Soc. Rev.* **2003**, *32*, 139−150.
(5) Giancarlo, L. C.; Flynn, G. W. *Acc. Chem. Res.* **2000**, *33*, 491−501.
(6) De Feyter, S.; Gesquière, A.; Abdel-Mottaleb, M. M.; Grim, P. C. M.; De Schryver, F. C.; Meiners, C.; Sieffert, M.; Valiyaveettil, S.; Müllen, K. *Acc. Chem. Res.* **2000**, *33*, 520−531.
(7) Giancarlo, L. C.; Flynn, G. W. *Annu. Rev. Phys. Chem.* **1998**, *49*, 297−336.
(8) Cyr, D. M.; Venkataraman, B.; Flynn, G. W. *Chem. Mater.* **1996**, *8*, 1600−1615.
(9) Claypool, C. L.; Faglioni, F.; Goddard, W. A.; Gray, H. B.; Lewis, N. S.; Marcus, R. A. *J. Phys. Chem. B* **1997**, *101*, 5978−5995.
(10) Faglioni, F.; Claypool, C. L.; Lewis, N. S.; Goddard, W. A. *J. Phys. Chem. B* **1997**, *101*, 5996−6020.
(11) Kim, K.; Matzger, A. J. *J. Am. Chem. Soc.* **2002**, *124*, 8772−8773.
(12) Samorí, P.; Severin, N.; Simpson, C. D.; Müllen, K.; Rabe, J. P. *J. Am. Chem. Soc.* **2002**, *124*, 9454−9457.
(13) Stabel, A.; Heinz, R.; Rabe, J. P.; Wegner, G.; De Schryver, F. C.; Corens, D.; Dehaen, W.; Süling, C. *J. Phys. Chem.* **1995**, *99*, 8690−8697.
(14) Kim, K.; Plass, K. E.; Matzger, A. J. *Langmuir* **2003**, *19*, 7149−7152.
(15) Kaneda, Y.; Stawasz, M. E.; Sampson, D. L.; Parkinson, B. A. *Langmuir* **2001**, *17*, 6185−6195.
(16) Stawasz, M. E.; Parkinson, B. A. *Langmuir* **2003**, *19*, 10139−10151.
(17) For a thorough treatment of crystal polymorphism, see: Bernstein, J. *Polymorphism in Molecular Crystals*; Clarendon Press: Oxford, 2002.
(18) Steed, J. W. *CrystEngComm* **2003**, *5*, 169−179.
(19) Several analyses of the frequency of occurrence of $Z' > 1$ have been undertaken: (a) Padmaja, N.; Ramakumar, S.; Viswamitra, M. A. *Acta Crystallogr., Sect. A* **1990**, *46*, 725−730. (b) Wilson, A. J. C. *Acta Crystallogr., Sect. A* **1993**, *49*, 795−806. (c) Brock, C. P.; Dunitz, J. D. *Chem. Mater.* **1994**, *6*, 1118−1127. (d) Steiner, T. *Acta Crystallogr., Sect. B: Struct. Sci.* **2000**, *56*, 673−676.

10.1021/ja0493446 CCC: $27.50

forces within each of them, allows much more rigorous examination and computational comparison.

Two-dimensional crystals are excellent models for understanding the factors determining selection of one possible crystal structure over another. Although the structure of physisorbed monolayers is influenced by substrate−molecule interactions, these can be expected to have a similar effect on related molecules adsorbed on the same substrate. Therefore, within a homologous series, the molecule−molecule interactions often dictate structure. This is especially true in cases where substrate−molecule interactions result in epitaxy: alignment of the two-dimensional crystal with the lattice of the substrate.[9,15,16,21] In the case of alkyl-substituted molecules, this epitaxy is ascribed to a near match in the periodicity of the graphite to the geometry of the alkyl chains.[8] Extensive studies have focused on the substituted *n*-alkanes, and the majority of molecules studied at the liquid−solid interface are decorated with long alkyl chains to increase ordering sufficiently to allow observation by scanning tunneling microscopy (STM).[7] Intermolecular bonding motifs common to three-dimensional crystals, such as hydrogen-bonding of carboxylic acids,[4−7,22−26] hydroxyl groups,[7−10,26,27] ureas,[4,28−32] and carbamates,[14,33] display similar bonding patterns in the two-dimensional structures. In fact, the two-dimensional crystals of some molecules are essentially equivalent to slices of the three-dimensional crystal.[8,34−37] In addition to probing the most fundamental aspects of the self-assembly events leading to crystal growth, there are a number of important practical applications of solution-formed physisorbed monolayers. These assemblies are relevant to organization of molecules on a substrate during lubrication,[38] fabrication of thin film organic electronic devices,[39] and the patterning of surfaces on the nanoscale.[4,23,40,41] These systems bear a close relationship to the process of heteronucleation which is vital in controlling three-dimensional crystallization.[42−44]

Chart 1. Structures of All Molecules Examined[a]

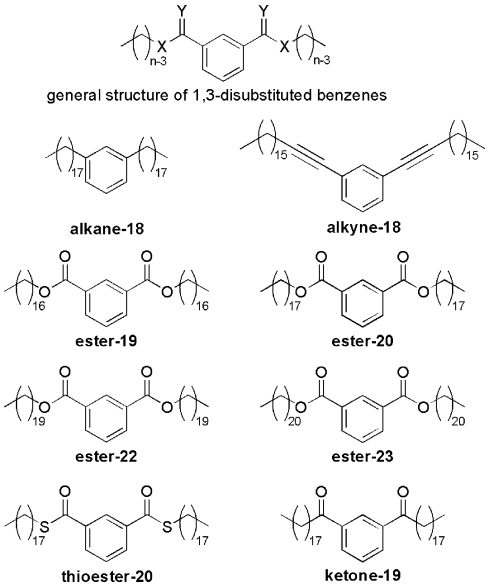

[a] The name given to each molecule is **functional group-*n***, where *n* is the number of non-hydrogen atoms in the backbone of each benzene substituent, as determined from the general structure given above.

Because a great deal of information about the determination of crystal packing can be obtained through the study of two-dimensional crystals of structurally related compounds, we employed STM and computational modeling to study the results of systematically changing the functionality in a series of 1,3-disubstituted benzenes (Chart 1). This particular series of compounds was chosen after the observation of an unprecedented one and a half symmetry-independent molecules ($Z' = 1.5$) in the two-dimensional crystal of 1,3-dinonadecanoylbenzene.[11] We have found that these 1,3-disubstituted benzenes exhibit unparalleled complexity in their two-dimensional packing. This great diversity is generated by alteration of just a few atoms. Molecular conformations, space groups, and Z' values are seen to vary based on subtle changes in molecular structure, and more than one packing motif is adopted by some molecules (vide infra).

Results and Discussion

General Observations. STM imaging in 1-phenyloctane solution was used to characterize physisorbed monolayers of (Chart 1): diheptadecyl isophthalate (**ester-19**); diheneicosyl

(20) Correlations between the existence of strong hydrogen bonds in a structure and $Z' > 1$ have been suggested: (a) Gavezzotti, A.; Filippini, G. *J. Phys. Chem.* **1994**, *98*, 4831−4837. (b) Brock, C. P.; Duncan, L. L. *Chem. Mater.* **1994**, *6*, 1307−1312. (c) Brock, C. P. *J. Res. Natl. Inst. Stand. Technol.* **1996**, *101*, 321−325. (d) Taylor, R.; Macrae, C. F. *Acta Crystallogr., Sect. B: Struct. Sci.* **2001**, *57*, 815−827. (e) Steed, J. W.; Sakellariou, E.; Junk, P. C.; Smith, M. K. *Chem.-Eur. J.* **2001**, *7*, 1240−1247. (f) Lehmler, H. J.; Robertson, L. W.; Parkin, S.; Brock, C. P. *Acta Crystallogr., Sect. B: Struct. Sci.* **2002**, *58*, 140−147. (g) Brock, C. P. *Acta Crystallogr., Sect. B: Struct. Sci.* **2002**, *58*, 1025−1031. (h) Gibson, S. E.; Ibrahim, H.; Steed, J. W. *J. Am. Chem. Soc.* **2002**, *124*, 5109−5116. (i) Kuleshova, L. N.; Antipin, M. Y.; Komkov, I. V. *J. Mol. Struct.* **2003**, *647*, 41−51. (j) Aitipamula, S.; Desiraju, G. R.; Jaskólski, M.; Nangia, A.; Thaimattam, R. *CrystEngComm* **2003**, *5*, 447−450.
(21) Buchholz, S.; Rabe, J. P. *J. Vac. Sci. Technol., B* **1991**, *9*, 1126−1128.
(22) Miura, A.; De Feyter, S.; Abdel-Mottaleb, M. M. S.; Gesquière, A.; Grim, P. C. M.; Moessner, G.; Sieffert, M.; Klapper, M.; Müllen, K.; De Schryver, F. C. *Langmuir* **2003**, *19*, 6474−6482.
(23) Hoeppener, S.; Chi, L.; Fuchs, H. *ChemPhysChem* **2003**, *4*, 494−498.
(24) De Feyter, S.; Gesquière, A.; Klapper, M.; Müllen, K.; De Schryver, F. C. *Nano Lett.* **2003**, *3*, 1485−1488.
(25) Olson, J. A.; Bühlmann, P. *Anal. Chem.* **2003**, *75*, 1089−1093.
(26) Wintgens, D.; Yablon, D. G.; Flynn, G. W. *J. Phys. Chem. B* **2003**, *107*, 173−179.
(27) Cai, Y.; Bernasek, S. L. *J. Am. Chem. Soc.* **2003**, *125*, 1655−1659.
(28) De Feyter, S.; Larsson, M.; Schuurmans, N.; Verkuijl, B.; Zoriniants, G.; Gesquière, A.; Abdel-Mottaleb, M. M.; van Esch, J.; Feringa, B. L.; van Stam, J.; De Schryver, F. *Chem.-Eur. J.* **2003**, *9*, 1198−1206.
(29) De Feyter, S.; Larsson, M.; Gesquière, A.; Verheyen, H.; Louwet, F.; Groenendaal, B.; van Esch, J.; Feringa, B. L.; De Schryver, F. *ChemPhysChem* **2002**, *3*, 966−969.
(30) Gesquière, A.; De Feyter, S.; De Schryver, F. C.; Schoonbeek, F.; van Esch, J.; Kellogg, R. M.; Feringa, B. L. *Nano Lett.* **2001**, *1*, 201−206.
(31) Gesquière, A.; Abdel-Mottaleb, M. M. S.; De Feyter, S.; De Schryver, F. C.; Schoonbeek, F.; van Esch, J.; Kellogg, R. M.; Feringa, B. L.; Calderone, A.; Lazzaroni, R.; Brédas, J. L. *Langmuir* **2000**, *16*, 10385−10391.
(32) De Feyter, S.; Grim, P. C. M.; van Esch, J.; Kellogg, R. M.; Feringa, B. L.; De Schryver, F. C. *J. Phys. Chem. B* **1998**, *102*, 8981−8987.
(33) Matzger, A. J.; Kim, K. *Polym. Mater. Sci. Eng.* **2003**, *89*, 825−826.
(34) De Feyter, S.; Gesquière, A.; Wurst, K.; Amabilino, D. B.; Veciana, J.; De Schryver, F. C. *Angew. Chem., Int. Ed.* **2001**, *40*, 3217−3220.
(35) Azumi, R.; Götz, G.; Debaerdemaeker, T.; Bäuerle, P. *Chem.-Eur. J.* **2000**, *6*, 735−744.
(36) Eichhorst-Gerner, K.; Stabel, A.; Moessner, G.; Declerq, D.; Valiyaveettil, S.; Enkelmann, V.; Müllen, K.; Rabe, J. P. *Angew. Chem., Int. Ed. Engl.* **1996**, *35*, 1492−1495.
(37) Yeo, Y. H.; McGonigal, G. C.; Thomson, D. J. *Langmuir* **1993**, *9*, 649−651.
(38) Bowden, F. P.; Tabor, D. *The Friction and Lubrication of Solids*; Clarendon Press: Oxford, 1954.
(39) Samorí, P.; Rabe, J. P. *J. Phys.: Condens. Matter* **2002**, *14*, 9955−9973.
(40) Hoeppener, S.; Wonnemann, J.; Chi, L.; Erker, G.; Fuchs, H. *ChemPhysChem* **2003**, *4*, 490−494.
(41) Abdel-Mottaleb, M. M. S.; Schuurmans, N.; De Feyter, S.; Van Esch, J.; Feringa, B. L.; De Schryver, F. C. *Chem. Commun.* **2002**, 1894−1895.
(42) Lang, M.; Grzesiak, A. L.; Matzger, A. J. *J. Am. Chem. Soc.* **2002**, *124*, 14834−14835.
(43) Mitchell, C. A.; Yu, L.; Ward, M. D. *J. Am. Chem. Soc.* **2001**, *123*, 10830−10839.
(44) Last, J. A.; Hillier, A. C.; Hooks, D. E.; Maxson, J. B.; Ward, M. D. *Chem. Mater.* **1998**, *10*, 422−437.

Table 1. Experimental and Computed Unit Cell Parameters for All Molecules Examined in All Phases Observed

			computed			experimental			
Z′	phase	molecule	*a* (Å)	*b* (Å)	α (deg)	*a* (Å)	*b* (Å)	α (deg)	space group
0.5	I	ester-19	59.9	8.8	90.0	61.2 ± 1.1	8.4 ± 0.1	90 ± 3	*cm*
	I	ester-23	70.4	8.9	90.0	73.0 ± 2.5	8.1 ± 0.4	89 ± 4	*cm*
	II	ester-20	62.5	8.8	90.0	65.6 ± 2.0	7.2 ± 0.2	87 ± 3	*p2mg*
	II	ester-22	67.5	8.8	90.3	70.0 ± 2.3	7.4 ± 0.2	92 ± 2	*p2mg*
1.0	III	alkane-18	52.3	6.8	41.0	52.4 ± 0.3	5.9 ± 0.1	44 ± 1	*p1*
	IV	ester-19	30.3	19.0	66.0	31.7 ± 0.7	21.6 ± 0.3	62 ± 1	*p2*
	IV	ester-23	35.4	18.5	67.2	39.1 ± 0.1	22.2 ± 0.1	63 ± 3	*p2*
	V	thioester-20	58.9	10.3	82.6	53.2 ± 1.8	11.2 ± 0.3	84 ± 2	*p2*
1.5	VI	ketone-19	122.7	13.6	90.0	128.1 ± 1.0	14.3 ± 0.3	91 ± 2	*cm*
2.0	VII	alkyne-18	26.3	21.8	74.2	26.1 ± 1.0	22.3 ± 0.6	75 ± 2	*p1*
5.0	VIII	ester-23	75.5	22.2	84.1	75.2 ± 0.7	25.6 ± 0.3	86 ± 1	*p1*

isophthalate (**ester-23**); dioctadecyl isophthalate (**ester-20**); dieicosyl isophthalate (**ester-22**); 1,3-dioctadecylbenzene (**alkane-18**); dioctadecyl dithiolisophthalate (**thioester-20**); 1,3-dinonadecanoylbenzene (**ketone-19**); and 1,3-dioctadec-1-ynylbenzene (**alkyne-18**). Each molecule is named with the functionality adjacent to the benzene ring, and then numbered according to the quantity of non-hydrogen atoms in the backbone of each benzene substituent (Chart 1).

All of the molecules examined formed two-dimensional crystals in one or more of the phases shown schematically in Figure 1. A phase is distinguished by its two-dimensional space group,[45] the number of molecules in the asymmetric unit (*Z′* value), and the conformation of the molecules in the asymmetric unit. The phases are numbered and discussed in order of increasing *Z′* values. For phases with identical *Z′*, the least symmetric phase is discussed first. The unit cell is defined by two length parameters (*a* and *b*) and the angle between them (α) (Table 1).

Image contrast and alkyl chain packing and orientation relative to the substrate were similar in all of the examined monolayers and comparable to substituted *n*-alkanes[7,9,10] and 1,4-dialkylbenzenes.[21,46−48] Chains of small bright spots, which smear into bright lines at low resolution, correspond to the hydrogen atoms on the alkyl chains oriented away from the substrate.[9,10] Alkyl chains are nearly commensurate with the underlying graphite lattice,[9,21] and are all oriented with the carbon backbones parallel to the graphite surface, as indicated by the "zigzag" pattern of the resolved hydrogens.[9,10] Neighboring alkyl chains are close packed; that is, adjacent chains are nestled such that each methylene fills the gap between two methylenes on the nearest chain, as shown in Figure 2a and b. In the STM images, large bright spots are indicative of aromatic rings.[21,46−50] The functional groups adjacent to the aromatic rings are not resolved due to their proximity to a portion of the molecule with a low tunneling barrier.[9]

***Z′* = 0.5.**

Phase I. 1,3-Diester-substituted benzenes with an odd number of carbons in each alkyl chain, both **ester-19** and **ester-23**, adopt phase I (Figure 1). Molecules are aligned in columns perpendicular to the alkyl chains, and these alkyl chains are interdigitated to give a close packed structure (Figure 2a and c). A half of a molecule (*Z′* = 0.5) is related to the rest of the two-dimensional crystal by the parallel mirror and glide planes in *cm* symmetry (Figure 2b and d). The spacing of the columns corresponds to the length of the alkyl chains. Due to the additional four methylene units in each alkyl chain for **ester-23**, which effects a computed difference in molecular length of 10.2 Å, the *a*-axis is expanded from 61.2 Å for **ester-19** to 73.0 Å for **ester-23** (Table 1).

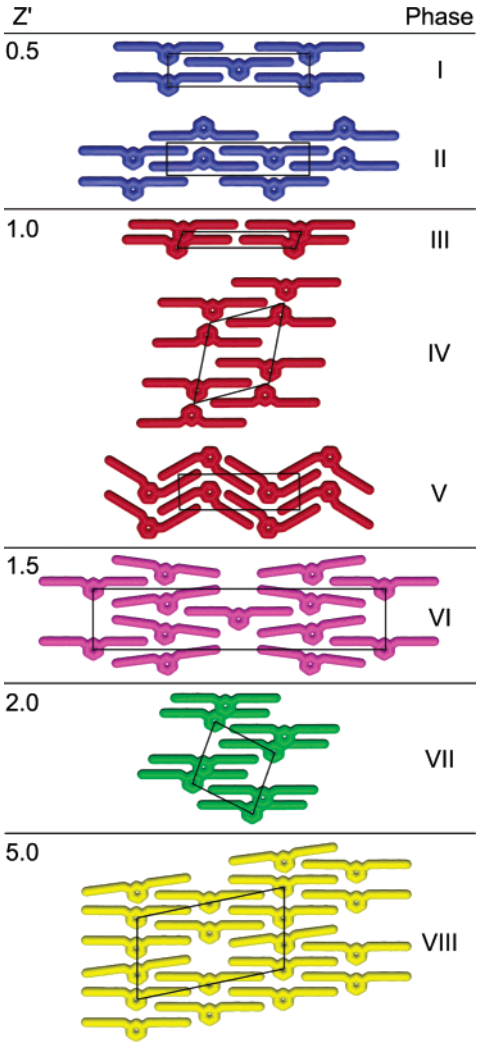

Figure 1. Schematic representation of all phases observed in two-dimensional crystals of 1,3-disubstituted benzenes, with unit cells indicated. These phases exhibit differing degrees of complexity, with varying space groups, numbers of molecules in the asymmetric unit (*Z′* values), and conformations.

(45) Hahn, T., Ed. *International Tables for Crystallography: Volume A Space-Group Symmetry*, 5th ed.; Kluwer Academic Publishers: Boston, 2002.
(46) Rabe, J. P.; Buchholz, S. *Phys. Rev. Lett.* **1991**, *66*, 2096−2099.
(47) Rabe, J. P.; Buchholz, S. *Science* **1991**, *253*, 424−427.
(48) Eng, L. M.; Fuchs, H.; Buchholz, S.; Rabe, J. P. *Ultramicroscopy* **1992**, *42*−*44*, 1059−1066.
(49) Lee, H. S.; Iyengar, S.; Musselman, I. H. *Langmuir* **1998**, *14*, 7475−7483.
(50) Lee, H. S.; Iyengar, S.; Musselman, I. H. *Anal. Chem.* **2001**, *73*, 5532−5538.

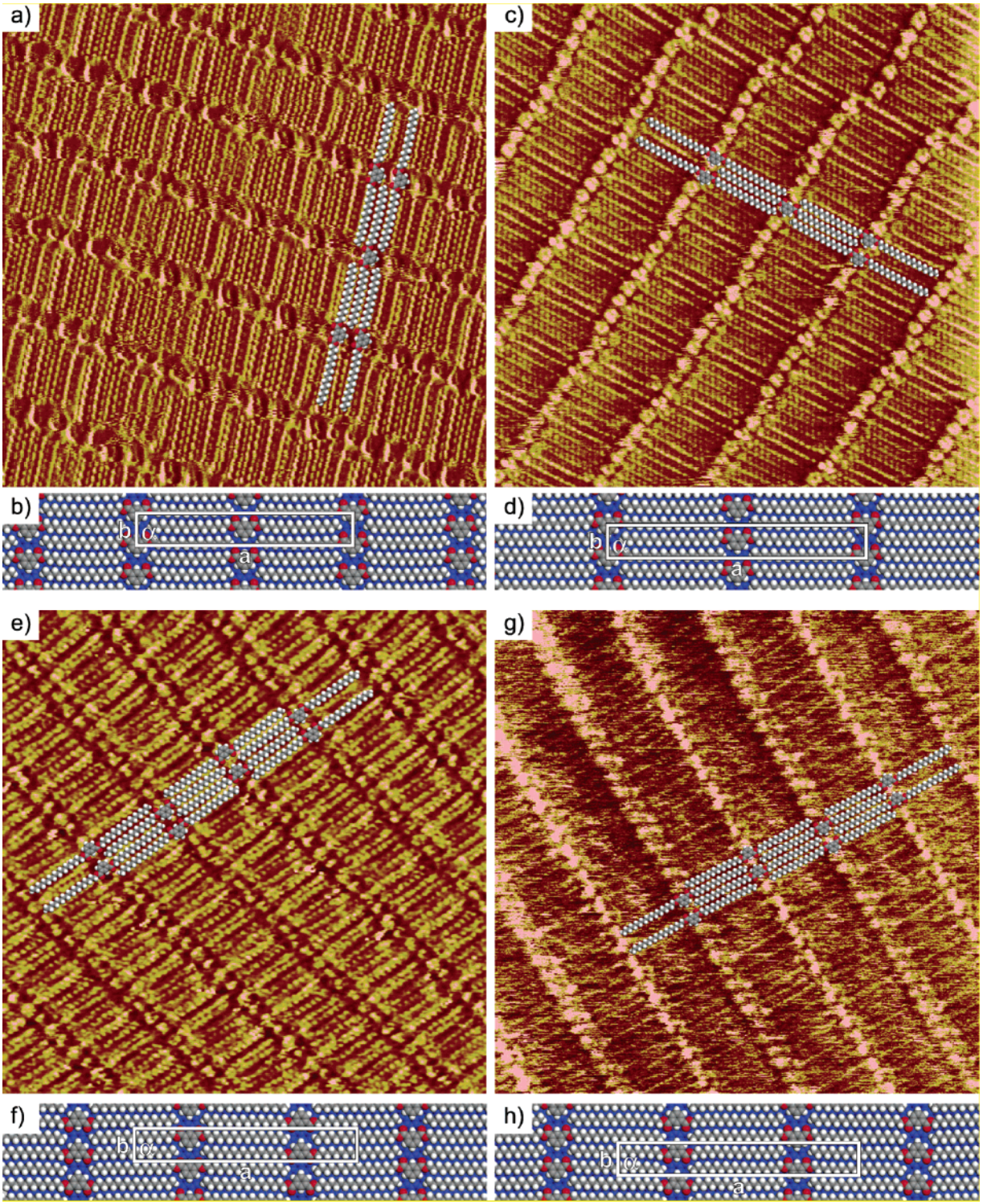

Figure 2. STM images (20×20 nm^2) with overlaid space-filling models of the molecules in the unit cell and computed models with unit cell outlined of all 1,3-disubstituted benzene compounds forming $Z' = 0.5$ phases: phase I (a−d) and phase II (e−h). **Ester-19** (a,b) and **ester-23** (c,d) form phase I, while **ester-20** (e,f) and **ester-22** (g,h) form phase II. The difference in contrast between columns of aromatic rings in the phase II STM images (e,g) and difference in orientation of the molecules in models (f,h) distinguish phases I and II.

Phase II. 1,3-Diester-substituted benzenes with an even number of carbons in the alkyl chains, **ester-20** and **ester-22**, form phase II (Figure 1). This structure is very similar to phase I except that the molecules in every other column face in the opposite direction. This is detected in the STM images by the slight variation in the contrast of the aromatic rings between adjacent columns that does not arise from the usual topographic or electronic effects (Figure 2e and g, also see Supporting Information). Similar orientation-induced contrast differences are observed in monolayers of long-chain diureas possessing carbonyl groups in an anti-configuration.[32] In phase II, half of a molecule ($Z' = 0.5$) is related to the entire structure by *p*2*mg* symmetry, defined by perpendicular mirror and glide planes (Figure 2f and h). As observed in phase I, the dependence of

the *a*-axis length on the number of carbons in the alkyl chain is present in phase II, with a 5.1 Å computed difference in molecular length causing an expansion in the *a*-axis from 65.6 Å for **ester-20** to 70.0 Å for **ester-22** (Table 1).

In the 1,3-diester-substituted benzenes, the selection of phase I over phase II is controlled by the parity of the number of carbon atoms composing the alkyl chains. This odd−even effect is a two-dimensional manifestation of the Principle of Close Packing delineated by Kitaigorodskii.[51,52] This principle states that the most dense modification of a molecular crystal gives the minimum free energy[52] and leads to the generalization that void space is unfavorable in crystals.[19c] This principle has been found to hold very well for hydrocarbon crystals where no strong directional intermolecular interactions occur and is also useful in understanding more functionalized systems.[52−54] Modeling the "odd" and "even" esters[55] in both phases I and II reveals differences in density introduced by the number of methylenes. An odd ester in phase I is positioned so that the methyl group of one molecule is directly beneath the methylene adjacent to the oxygen of the molecule above it. This permits maximum alkyl chain contact. Shortening the alkyl chain by one carbon leaves a space at the end of the chain, creating a lower density structure. A denser structure that maintains close packing of the alkyl chains is obtained by an inward shift by two methylenes, but this leads to unfeasibly close contacts with the aromatic ring. Alternation of molecular orientation in the adjacent columns, as in phase II, positions the methyl group between these two extremes. This results in the densest possible structure without introducing strongly repulsive close contacts. The calculated densities[56] and corresponding lattice energy differences between phase I and phase II clearly agree with the correlation between density and stability (see Supporting Information). Phase I is calculated to be more dense than phase II for both **ester-19** and **ester-23**, with density differences of 0.10 and 0.08 Da $Å^{-2}$, respectively, and more stable than phase II by 1.69 and 1.71 kcal mol^{-1}, respectively, according to molecular mechanics (see Experimental Section). The opposite is seen with the even esters, **ester-20** and **ester-22**, where phase II is more dense than phase I by 0.09 Da $Å^{-2}$ for both and more stable than phase I by 1.70 and 1.72 kcal mol^{-1}, respectively.

$Z' = 1.0$.

Phase III. Alkane-18 forms phase III (Figure 1), the only phase where columns do not interdigitate in this series (Figure 3a). Every **alkane-18** is close packed with two molecules on either side, each offset by four methylenes. This offset results in lines of aromatic rings at 44° angles relative to the alkyl chains. The spacing between bright columns measured along the alkyl chain direction is approximately equal to the length of the molecule, 52.4 Å. This stands in contrast to interdigitated phases, where this spacing is approximately half of the length of the molecule. There is a dim trough halfway between the lines of aromatic rings due to the space between the methyl end groups. The 5.9 Å periodicity between molecules within the column and 4.1 Å spacing between molecules perpendicular to their long axis indicate that the alkyl chains are close packed. These spacings are considerably less than the van der Waals diameter of a benzene ring, suggesting that the benzene rings partially desorb to avoid unphysically close contacts. Each molecule ($Z' = 1.0$) is related only by translation, giving *p*1 symmetry (Figure 3b, Table 1). This structure is similar to the two-dimensional crystals of 1,4-dialkylbenzenes.[21,46−48] Both **alkane-18** and the *para*-substituted alkyl benzenes form angled noninterdigitated columns of molecules. The *para*-substituted molecules, however, have a two-methylene offset between neighboring molecules, rather than four. This difference in offset is a result of the change in the geometry of the alkyl chains and their ability to close pack while accommodating the bulk of the benzene ring. The *para*-arrangement can easily accommodate close packing of the alkyl chains by adopting a geometry where the chains are parallel to each other and the benzene ring is nearly perpendicular to the surface. This conformation has a kink at the benzene ring, and the offset between molecules accommodates this and produces favorable slipped face-to-face interactions between aromatic rings. In the *meta*-arrangement (**alkane-18**), the two-alkyl chains on the same molecule are parallel and collinear. A two-methylene offset, which might have been expected to provide favorable π-stacking, is not seen. The distortion around the benzene ring makes it difficult for the two rings to come close enough for this interaction. A four-methylene offset makes a weak C−H$\cdots\pi$ interaction possible without interference from the distorted geometry.

Desorption of the benzene ring from the surface controls whether interdigitation occurs in this series of molecules. Molecules lay flat and interdigitate in phases I and II, unlike phase III where the aromatic ring is desorbed and there is no interdigitation. Periodic simulations using molecular mechanics (see Experimental Section) of **alkane-18** monolayers reveal that the desorption in phase III is accommodated by the contortion of several bonds, most notably the connection between the alkyl chains and benzene ring. Density functional theory (DFT) calculations (see Experimental Section) on a model ester, methyl benzoate, and a model alkane, propyl benzene, show that torsional rotation about the bond between the benzene ring and substituent away from 0° (flat) is energetically favorable for the alkane but not the ester (see Supporting Information). At 52.5°, a value close to the maximum torsion angle observed in the periodic simulation of **alkane-18** (52.9°), the model alkane is stabilized by 0.39 kcal mol^{-1} relative to the planar structure, whereas the model ester is destabilized by 4.1 kcal mol^{-1}. This barrier to rotation in the esters disfavors benzene ring desorption from the surface, leading to phases I and II, which are the densest possible phases wherein the molecules lie flat. Methyl thiobenzoate, a **thioester-18** model, and propanoyl benzene, a **ketone-19** model, are likewise destabilized at 52.5° by 2.4 and 3.8 kcal mol^{-1}, respectively. Thus, all carbonyl-containing molecules are expected to lie flat on the graphite substrate (vide infra).

Phase IV. In addition to adopting phase I, the odd esters, **ester-19** and **ester-23**, form another packing motif, phase IV (Figures 1 and 3c). This phase occurs in small domains that coexist with the dominant motif, phase I (Figure 3e, see

(51) Kitaigorodskii, A. I. *Acta Crystallogr.* **1965**, *18*, 585−590.
(52) Kitaigorodskii, A. I. *Organic Chemical Crystallography*; Consultants Bureau: New York, 1959.
(53) Burger, A.; Ramberger, R. *Mikrochim. Acta* **1979**, *2*, 259−271.
(54) Burger, A.; Ramberger, R. *Mikrochim. Acta* **1979**, *2*, 273−316.
(55) The 1,3-diester-substituted benzenes are described as "odd esters" or "even esters" on the basis of the parity of the number of carbons in each alkyl chain.
(56) The calculated densities were obtained by multiplication of the molecular weight (Da) by the number of molecules in the unit cell, followed by division by the surface area of the models in square angstroms ($Å^2$).

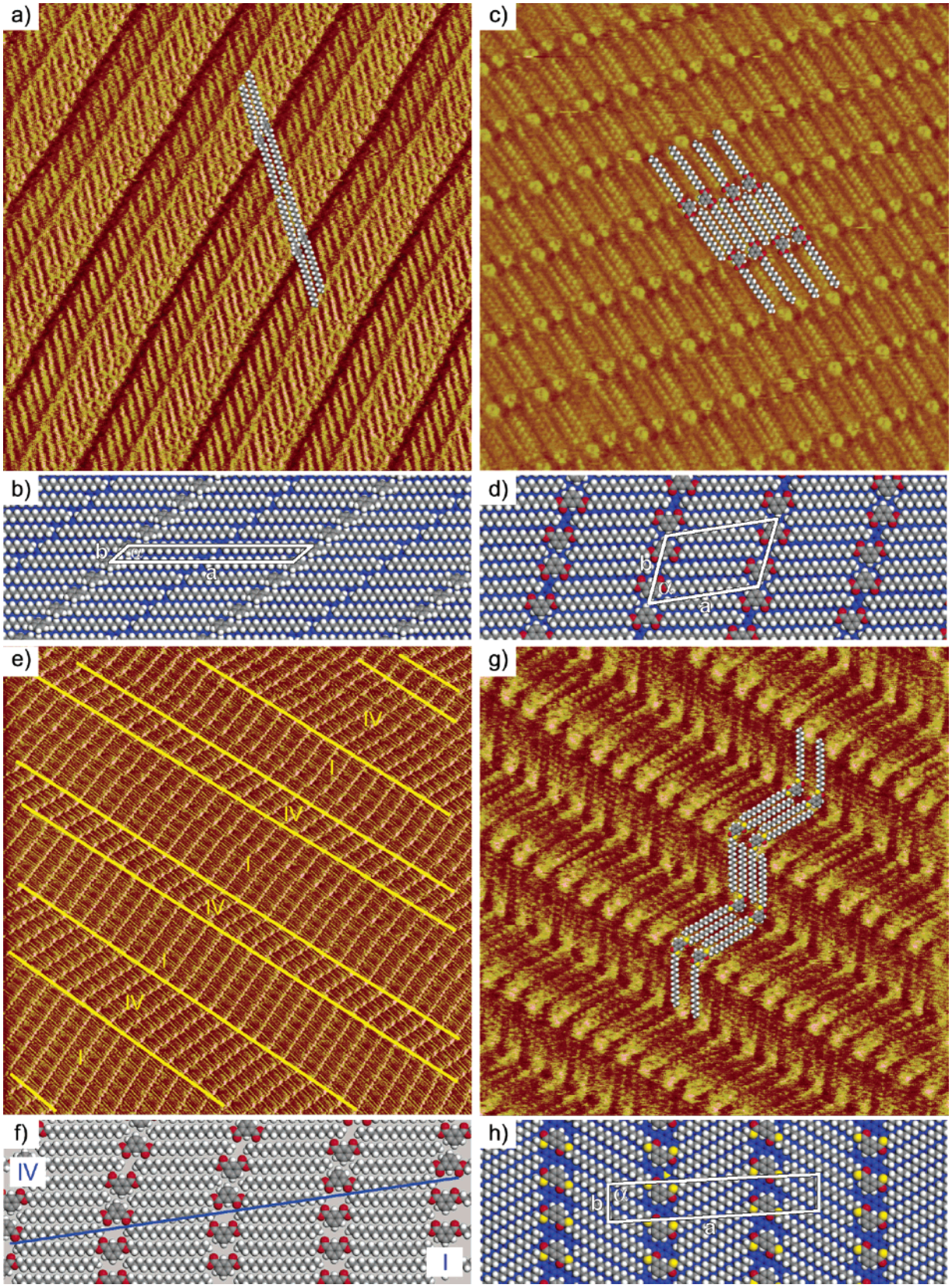

Figure 3. STM images (20×20 nm^2) with overlaid space-filling models of the molecules in the unit cell and computed models with unit cell outlined of 1,3-disubstituted benzene compounds forming $Z' = 1.0$ phases: **alkane-18** in phase III (a,b), **ester-19** in phase IV (c,d), and **thioester-20** in phase V (g,h). Phase III (a,b) is the only phase in this series which does not interdigitate. **Ester-19** (c,d) forms a pseudopolymorph, phase IV, in addition to phase I. This pseudopolymorph also forms in **ester-23** (e) and coexists with phase I on the surface forming uninterrupted bright lines of aromatic rings. The area shown in this image is particularly rich in phase IV. The smooth interface between phases I and IV (f) promotes formation of phase IV. Phase V (g−h) is the only motif consisting of molecules with alkyl chains at 120° angles.

Supporting Information). Strictly speaking, phase IV does not bear a true polymorphic relationship to phase I. Each unit cell has a different area; therefore, the stoichiometry between the adsorbed molecules and the graphite surface differs between phases. This is indicative of a pseudopolymorphic relationship.[57] In phase IV, molecules form pairs where the aromatic rings point inward and are offset by one methylene. These pairs then interdigitate, producing lines of aromatic rings at a 62° angle with respect to the alkyl chains. Each molecule ($Z' = 1.0$) is related to the others through two-fold rotation axes defining $p2$ symmetry (Figure 3d, Table 1).

Phase IV is a less stable pseudopolymorph than phase I, the formation of which is induced by the reduction in interfacial energy it provides. Analysis of the intermolecular interactions, and the observation that it is the minority phase on the surface, demonstrate that phase IV is less stable than phase I. In phase IV, the two-fold rotation axis places the hydrogens at the 5 position of the aromatic rings very close to each other, creating unfavorable steric interactions. According to molecular mechanics computations, phase IV is less stable than I by 2.3 kcal mol^{-1} primarily due to destabilization in the nonbonded terms. Phase IV is likely formed to reduce the interfacial energy between offset domains of phase I. The smooth interface between domains of these phases is seen in large-scale images (Figure 3e), where the bright lines of aromatic rings are continuous throughout the entire 100 × 100 nm^2 area. An interface between two offset domains of phase I breaks this column of aromatic rings and results in unstable areas where close packing is not possible. Because of the angle between its column and propagation directions, phase IV provides a smooth transition between offset domains of phase I, eliminating this less stable boundary (Figure 3f). Supporting this mechanism is the fact that phase IV persists after initial Ostwald ripening,[6,58] the process by which small domains merge into larger ones, is complete. Because the driving force for this process is the elimination of unstable interfaces, this slow disappearance supports the role of phase IV as a stabilizing transition region between domains of phase I.[59] This stands in contrast to cases where a kinetically stable form initially appears, then transforms to a thermodynamically stable form.[14] Another way in which phase IV can lower the interfacial energy is to form a smooth boundary between domains that are at 60° angles to each other (see Supporting Information). Similar changes in a two-dimensional crystal to fill empty space at a domain boundary have been observed, but usually this change comes in the form of disturbing the dominant phase, not inducing formation of a new phase.[14,60]

Phase V. The 120° angle between the alkyl chains of **thioester-20** in phase V (Figure 1) distinguishes this phase from others seen in the series, all of which have 180° angles between alkyl chains (Figure 3g). The 120° angle between the alkyl chains allows nearly commensurate interaction with two different directions of the graphite substrate, a packing often seen in *n*-alkanols.[7−10,26,27] Every molecule of **thioester-20** is close packed with four molecules, two from each adjacent column. Each of these molecules ($Z' = 1.0$) is related by a two-fold rotation axis, giving rise to $p2$ symmetry (Figure 3h, Table 1). This symmetry element dictates that every other column contains oppositely oriented molecules; that is, the 120° angle between alkyl chains makes a "V-shape" that opens up in one column and down in the next. As seen in phase II, this arrangement results in an orientation-induced alternation in contrast.

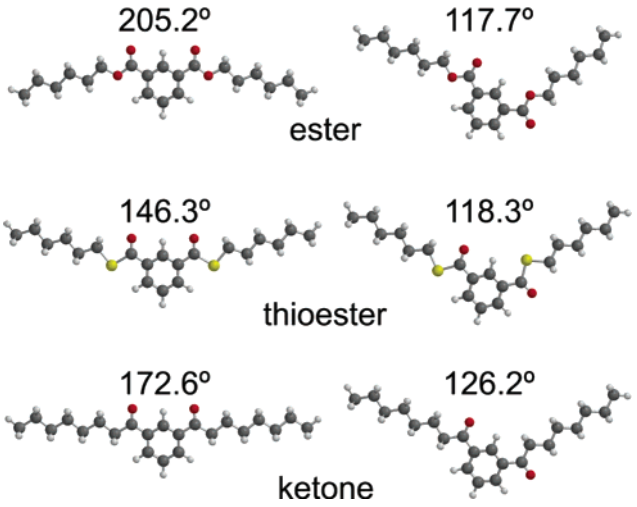

Figure 4. DFT-calculated equilibrium geometries of short-chain analogues of **ester-20** (dihexyl isophthalate), **thioester-20** (dihexyl dithiolisophthalate), and **ketone-19** (1,3-dioctanoylbenzene) with carbonyls pointing toward the 2 position of the benzene rings and in opposite directions. Formation of phase II, which requires a 180° angle between alkyl chains, is more difficult to achieve for the thioester due to its smaller preferred alkyl chain angle. Torsion rotation allows the thioester to have a 120° angle between alkyl chains, thus forming phase V and maintaining commensurateness with the graphite. The angle difference between the ester and ketone is less pronounced, but induced angle strain may contribute to selecting against formation of phase VI for **ester-19**.

The difference in two-dimensional structure between **thioester-20** and **ester-20**, molecules having essentially the same size and similar functionality, results from a slight difference in their minimum energy conformation. The geometry of **thioester-20** in phase V differs from that of **ester-20** in phase II in that there is a 180° twist of the torsion angle between the carbonyl group and the benzene ring on one of the alkyl chains, resulting in the 120° angle between them. The effect of this 180° twist on the angle between the alkyl chains is seen in the calculated minimum energy geometries of short-chain analogues of **ester-20** and **thioester-20**, each with six carbons per alkyl chain (Figure 4), and is caused by the difference in the preferred angle about the oxygen of the ester and the sulfur of the thioester. When the carbonyl groups point in opposite directions, the angle formed by the alkyl chains is 118° for both molecules. When both carbonyl groups point toward the 2 position of the benzene ring, these angles are 205° and 146° for dihexyl isophthalate and dihexyl dithiolisophthalate, respectively. Due to the greater deviation from 180° observed for the thioester, the energy required to force the alkyl chains of **thioester-20** to 180° is greater (2.2 kcal mol^{-1} for dihexyl dithiolisophthalate vs 1.1 kcal mol^{-1} for dihexyl isophthalate). Accordingly, **thioester-20** adopts a more open structure[56] (2.48 Da Å^{-2} for phase II vs

(57) Although numerous definitions have been offered for the term pseudopolymorphism, as reviewed by Bernstein,[17] we use the definition from Nangia, A.; Desiraju, G. R. *Chem. Commun.* **1999**, 605−606 that refers to "crystalline forms that differ in the nature or stoichiometry of included solvent molecules". Applying this definition to two-dimensions implies that monolayers of a given compound that differ in stoichiometry with the surface are pseudopolymorphs.

(58) Stabel, A.; Heinz, R.; De Schryver, F. C.; Rabe, J. P. *J. Phys. Chem.* **1995**, *99*, 505−507.

(59) In this context, it is interesting to note that a smooth interface surrounding a thermodynamically unstable domain prolongs its existence.[60]

(60) Baker, R. T.; Mougous, J. D.; Brackley, A.; Patrick, D. L. *Langmuir* **1999**, *15*, 4884−4891.

2.32 Da Å^{-2} for phase V) on the surface to pack in a lower energy conformation. Further support for the role of intrinsic geometric preference of the ester and thioester functional groups in determining monolayer packing structure is available by analysis of crystal structures in the Cambridge Structural Database (CSD). Ester and thioester functionalities adjacent to benzene rings were found to have distinct angles about the heteroatoms, 117° and 101°, respectively, with narrow distributions that showed minimal overlap (standard deviations of ~2°). The corresponding values from DFT for the short-chain model compound are 116° and 98.5° for the ester and thioester, respectively (see Supporting Information).

$Z' = 1.5$.

Phase VI. Ketone-19 molecules reside in two distinct environments in phase VI (Figure 1), leading to symmetry-independent molecules in the unit cell.[11] Two different columns of molecules exist on the surface: column A contains twice as many molecules as adjacent column B (Figure 5a). Molecules in column A are tilted such that the alkyl chains of two molecules close pack on one side of the aromatic rings, but are separated by a molecule from column B on the other. High-resolution STM images reveal the difference in tilt of each molecule in column A (see Supporting Information). One molecule in column A is related to the others by a glide plane, whereas one molecule in column B lies on a mirror plane, resulting in $Z' = 1.5$ and *cm* symmetry (Figure 5b, Table 1).

Although **ketone-19** is similar in size and functionality to **ester-19**, it forms phase VI rather than phase I, despite the fact that phase I would be more dense: phase VI has a density of 2.29 Da Å^{-2}, but computation of **ketone-19** in phase I finds a greater density (2.39 Da Å^{-2}). Selection of this phase is driven by the formation of a more electrostatically favored arrangement. Molecules in column A of phase VI are in more intimate contact with each other than molecules in column B, the latter having a similar conformation and arrangement of molecules as in phase I. Weak hydrogen bonds form within column A between one carbonyl group of a given molecule and an aromatic hydrogen on a neighboring molecule (see Supporting Information). The computed C−H···O distance of 2.5 Å and angle of 162.3° are well within the values typically observed in three-dimensional crystals.[61] Each molecule in column A has two hydrogen bonds, one where it is the donor and one where it is the acceptor, giving rise to an infinite chain. As both ester and ketone functionalities can form these hydrogen bonds, the few properties distinguishing **ketone-19** and **ester-19** must be responsible for the difference in two-dimensional crystal structure. The more polarized ketone functional group has a more electrostatically favorable (stronger) interaction with aromatic hydrogens.[62] These electrostatic forces stabilize phase VI by ~1 kcal mol^{-1} more for the ketone than the ester as judged by comparison of the differences in energy terms between the periodic simulations of these phases. In conjunction with the weaker hydrogen bond that would form for **ester-19** in phase VI, the angle strain required in **ester-19** to accommodate this phase is slightly greater (Figure 4).

(61) For typical C−H···O bond geometries as well as a review of these types of weak hydrogen bonds, see: Desiraju, G. R.; Steiner, T. *The Weak Hydrogen Bond In Structural Chemistry and Biology*; Oxford University Press: Oxford, 1999.

(62) A similar difference in the strength of hydrogen bonds to amines from ketone and ester donors has been observed: Ziao, N.; Laurence, C.; Le Questel, J. Y. *CrystEngComm* **2002**, *4*, 326−335.

$Z' = 2.0$.

Phase VII. Alkyne-18 forms phase VII (Figure 1), composed of two distinct molecules (Figure 5c). One of these molecules lies flat on the surface, while the other is offset by four methylenes and positioned so that the alkyl chains are in contact. This forces the aromatic ring of the second molecule to partially desorb from the surface to avoid close contacts with the first molecule, a situation analogous to phase III. The height difference between the two rings is discernible from the STM image (see Supporting Information). Each asymmetric pair is interdigitated with adjacent units, resulting in columns of aromatic rings at 123° angles to the alkyl chains, due to the offset between the two molecules. The raised ring comes close enough to the methylene hydrogen beneath it that stabilization by a C−H···π interaction is possible, and this may contribute energetically to driving the offset between molecules in the asymmetric unit. Avoidance of a repulsive interaction between the aromatic rings and the triple bond could also drive this offset. Two molecules of different conformation ($Z' = 2.0$) are translated to generate the entire two-dimensional structure of phase VII (Figure 5d, Table 1); thus it has *p*1 symmetry.

$Z' = 5.0$.

Phase VIII. Ester-23 formed phase VIII (Figure 1) after a short voltage spike (10 V) to the STM tip while imaging phase I (Figure 5e). Phase VIII forms two different columns that interdigitate such that the alkyl chain length separates the lines of aromatic rings. Column B has two molecules for every three molecules in column A. Periodic spaces between the molecules in column A and B are reproduced in the simulation of this phase (Figure 5f). Every third molecule in column A is curved in the same sense, restricting the symmetry to space groups without mirror planes or glide planes. Furthermore, there are no rotation axes. Therefore, molecules with the same conformation, such as the two molecules in column B, cannot be related by symmetry. The five distinct molecules ($Z' = 5.0$) translate with *p*1 symmetry to generate the two-dimensional crystal (Figure 5f, Table 1).

Phase VIII is a metastable pseudopolymorph that accommodates some hydrogen bonding while minimizing the angle strain in most of the molecules. Molecular mechanics calculations show that phase VIII is less stable than phase I by 2.42 kcal mol^{-1} due primarily to a reduction in the van der Waals contacts (2.11 kcal mol^{-1}) and additional angle strain (0.78 kcal mol^{-1}). Column A contains a weak hydrogen-bonding pattern (C−H···O distances of 2.6 Å and angles of 155.0° and 127.3°)[61] similar to that seen in phase VI, but it is restricted to three molecules as opposed to an infinite chain (see Supporting Information). Phase VIII can be viewed as phase I with an additional molecule squeezed into every other column. All molecules, except the one curved molecule, have nearly 180° angles between the alkyl chains, like in phase I. This curved molecule enables hydrogen bonding between the two molecules surrounding it. The STM image shows that the gap between the aromatic rings is much less on either side of the curved molecule than between the straighter molecules in column A. The appearance of this phase, followed by its disappearance, indicates that it is a kinetically favored form that transforms to the thermodynamically favored phase I. Despite extensive experimentation, generation of this phase has not been repeated. However, it clearly was possible to access this packing motif

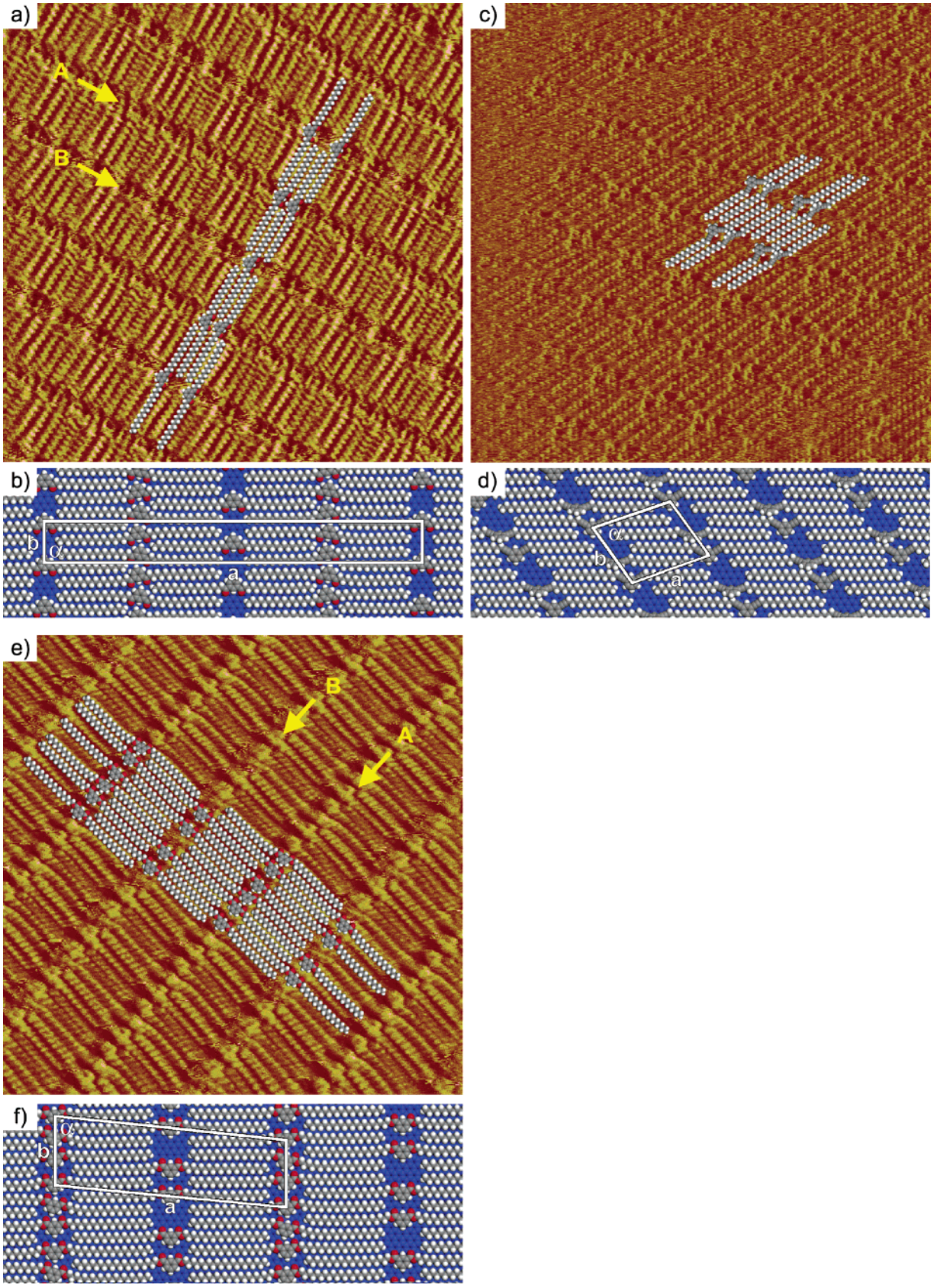

Figure 5. STM images (20 × 20 nm^2) with overlaid space-filling models of the molecules in the unit cell and computed models with unit cell outlined of all 1,3-disubstituted benzene compounds forming $Z' > 1$ phases: **ketone-19** in phase VI (a,b), **alkyne-18** in phase VII (c,d), and **ester-23** in phase VIII (e,f). Phase VI (a,b) consists of two distinct columns, with twice as many molecules in column A as in B. Phase VII (c,d) has two different molecules with the aromatic ring of one molecule desorbed from the surface. Phase VIII (e,f) is a pseudopolymorph of **ester-23** with five nonsymmetry related molecules.

(Figure 5e). Thus, it is a two-dimensional analogue of three-dimensional disappearing polymorphs.[63]

Implications

The 1,3-disubstituted benzenes offer a unique opportunity to investigate $Z' > 1$, the effect of chemical functionality on crystal packing, and (pseudo)polymorphism in both two- and three-dimensional crystals. In this series, structures exhibiting $Z' > 1$ were formed with unprecedented frequency, and drastic changes in crystal packing resulted from even subtle changes in chemical functionality. In addition, pseudopolymorphism was observed for several of the molecules, and the structure-determining interactions were identified. Determination of the interactions which lead to these phenomena was possible in two-dimensional crystals of the 1,3-disubstituted benzenes because of the reduction in the total number of factors influencing adoption of a given crystal structure coupled with the ability to compare closely analogous molecules.

The occurrence of more than one molecule in the asymmetric unit of a crystal is a phenomenon of interest from a fundamental standpoint, because the factors leading to its occurrence are not well understood, and for the practical reason that it greatly complicates the prediction of crystal packing. The vast majority of three-dimensional organic crystal structures (87.0%) have Z' of 1 or 0.5, but 10.8% have $Z' > 1$.[19d] Despite the importance of this phenomenon, there exists no general theory describing its incidence in three-dimensions. However, $Z' > 1$ has been correlated with irregular molecular shape and frustration between the requirements of close packing and satisfaction of strong intermolecular forces.[18,20] An increase in the likelihood of large Z' values has been associated with molecules containing strongly interacting functionalities such as nucleosides, nucleotides, and alcohols.[18] For example, studies of monoalcohols and *vic*-diols found an increased tendency to form crystals with $Z' > 1$ to maximize hydrogen bonds between hydroxyl groups.[20] Not all of these molecules formed $Z' > 1$ structures, but were inclined to do so when geometric factors made satisfying hydrogen bonds difficult: 40% of monoalcohols examined had Z' greater than 1,[20b] as did 33% of the *vic*-diols.[20g]

Monolayers of 1,3-disubstituted benzenes provide a unique opportunity to study the formation of symmetry-independent molecules in a unit cell. The occurrence of $Z' > 1$ is far more rare in two-dimensional crystals than in three-dimensional crystals.[64] This frequency difference is especially glaring when the likely underrepresentation of $Z' > 1$ structures in the CSD is taken into account. The observed rate of occurrence of large Z' values in three-dimensions is artificially lowered by the complications inherent in determining crystal structures with multiple molecules in the asymmetric unit and the possibility of solving these structures with fewer symmetry-independent molecules than are actually present. Although the former problem is not encountered in STM because it directly images the crystal, low-resolution STM images may be interpreted as possessing higher symmetry or smaller unit cells than actually present. It was only after more than 10 years of STM observation of physisorbed monolayers[21,46,47,65] at the solution−solid interface with $Z' = 0.5$ or 1.0 that $Z' > 1$ was reported.[11,12,66,67] The present study more than doubles the number of documented cases of high Z' values in these types of monolayers and contains the only examples of conformationally distinct molecules in the asymmetric unit. Monolayers with 0.5 and 1.0 molecule in the asymmetric unit were, as in the vast majority of previous studies, more common. However, $Z' = 1.5$, 2.0, and 5.0 monolayers were also formed. Although 9.4% of structures in three-dimensions have $Z' = 2.0$, $Z' = 5.0$ has been reported in less than 0.02% of three-dimensional crystal structures in the CSD.[19d] Of course, these numbers are not expected to hold in two-dimensional crystals, and considerably more data are needed for definitive trends to emerge. Perhaps the additional rarity of $Z' > 1$ in two-dimensional crystals reflects a bias against adsorption to the surface sufficient to allow structure determination by those molecules with difficulty in satisfying the many factors determining packing as well as the constraint of the surface.

Given the extreme rarity of $Z' > 1$ at the liquid−solid interface, the large variation in Z' values of the 1,3-disubstituted benzenes provides a unique opportunity to investigate the origin of multiple molecules in the asymmetric unit, through comparison of the $Z' > 1$ to the $Z' \leq 1$ motifs and comparison of the 1,3-disubstituted benzenes to previously examined molecules. Within the series, $Z' > 1$ occurs as a result of a compromise between close packing and weak directional intermolecular interactions. All of the phases with $Z' > 1$ have lower densities than other possible motifs, but satisfy some kind of directional intermolecular bonding. **Ketone-19** (phase VI, $Z' = 1.5$) and **ester-23** (phase VIII, $Z' = 5.0$) form structures with $Z' > 1$ as this allows satisfaction of C−H···O bonds at the cost of reduced density and increased angle strain. **Alkyne-18** (phase VII, $Z' = 2.0$) likely forms a low-density structure with $Z' > 1$ either to satisfy C−H···π bonds or to avoid π···π repulsion. The 1,3-disubstituted benzenes may have formed $Z' > 1$ structures, unlike most molecules examined thus far, because of the intermediacy of the strength of these interactions. Typically, solution-formed physisorbed monolayers are organized by very strong or very weak forces. Strong interactions are essentially always satisfied in two-dimensions, thereby dictating structure. The energies of weak hydrogen

(63) The difficulty in controlling and reproducing the formation of some metastable polymorphs is a widely recognized phenomenon in the field of three-dimensional crystallization: Dunitz, J. D.; Bernstein, J. *Acc. Chem. Res.* **1995**, *28*, 193−200.

(64) It might have been expected that the requirement of adsorption to the surface would add to frustration of close packing, making $Z' > 1$ more common in two-dimensional crystals. Surface reconstructions involving ionic or covalent crystals often display extremely large numbers of inequivalent sites. However, experiments carried out on physisorbed monolayers reveal that the additional restriction of two-dimensionality due to the surface does not add substantially to the appearance of $Z' > 1$, as is apparent from the comparison of the statistics of two- and three-dimensional crystals. This may be observed because of the relatively weak and nondirectional interactions involved with these physisorbed monolayers.

(65) McGonigal, G. C.; Bernhardt, R. H.; Yeo, Y. H.; Thomson, D. J. *J. Vac. Sci. Technol., B* **1991**, *9*, 1107−1110.

(66) A few examples of $Z' > 1$ in two-dimensional crystals have been observed by other preparation methods. An example of $Z' = 2$ can be found in vapor-formed two-dimensional crystals of nickel(II) octaethylporphyrin: Scudiero, L.; Barlow, D. E.; Hipps, K. W. *J. Phys. Chem. B* **2002**, *106*, 996−1003. An example of $Z' > 2$ can be found in solvent-evaporated two-dimensional crystals of alkyl-substituted triphenylenes: Wu, P.; Zeng, Q. D.; Xu, S. D.; Wang, C.; Yin, S. X.; Bai, C. L. *ChemPhysChem* **2001**, *2*, 750−754. Monolayers formed by these techniques have fewer opportunities to reorganize as compared to monolayers remaining in solution for extended periods, and thus may be kinetically favored phases, while monolayers imaged at the solution−solid interface are more likely to be the thermodynamically favored structure.

(67) Liquid crystals of alkylcyanobiphenyls form multiple asymmetric molecules on graphite that can be observed by STM. However, the observed layer is not a two-dimensional crystal because it is part of a structure with three-dimensional order. Frommer, J. *Angew. Chem., Int. Ed. Engl.* **1992**, *31*, 1298−1328.

bonds, however, are on the order of van der Waals forces, leading to competition between satisfying directional interactions and close packing. Adding to the likelihood of $Z' > 1$ as compared to previous studies, is the awkward shape of the 1,3-disubstituted benzenes which further frustrates close packing. This is not by itself enough to cause $Z' > 1$, as seen by the geometric similarity of molecules within the series, most of which do not form $Z' > 1$ motifs. These considerations suggest that $Z' > 1$ will become more common in two-dimensional crystals with expansion of the complexity of examined molecules. Indeed, this is likely playing a role already, as indicated by the recent observation of another $Z' > 1$ structure.[12] The difference between identified factors contributing to $Z' > 1$ in two- and three-dimensional crystals seems to be the magnitude of the competing interactions.[18] In three-dimensional crystals, $Z' > 1$ has been associated with strong intermolecular interactions which can overcome close packing.[18,20] Comparison with two-dimensional crystals indicates that rather than the absolute strength of the intermolecular bonds determining $Z' > 1$ structures, the relative strengths are more important. This provides an important caveat in the development of predictive rules from structures with $Z' > 1$. It is not solely the nature of the directional interactions that leads to $Z' > 1$, but a more complex relationship involving the type and strength of forces favoring close packing.

The diversity of packing motifs in the 1,3-disubstituted benzenes is remarkable considering the small changes in functionality. In the cases of *n*-substituted alkanes,[7,9,68,69] anthrone derivatives,[13] and halogen-substituted phenyl octadecyl ethers,[49,50] changes in functionality result in switching between parallel and herringbone motifs, adoption of head-to-tail or head-to-head configurations, and varying offsets between molecules. By contrast, the 1,3-disubstituted benzenes have dramatic differences in conformation, as well as differences in the number of symmetry-independent molecules and orientation to the surface. In three-dimensional crystals, it is commonly observed that dramatic crystal structure changes are a consequence of subtle changes in molecular structure; thus the structural response to functionality in the 1,3-disubstituted benzenes illustrates that two-dimensional crystals are excellent models for three-dimensional phenomena. Changing functionality is a smaller perturbation on intermolecular forces in two-dimensions because there are fewer interactions operating; thus these changes can be well understood. When each molecule was modeled in a given phase, it was found that most of the phases were local energy minima for similar molecules, with small calculated energy differences selecting among them. The determination of most motifs was based on a competition between close packing and distortion of the equilibrium geometry of the individual molecules accommodating electrostatic interactions. This is exemplified by selection of different phases by the ester- and ketone-containing molecules based on the strength of the hydrogen-bond acceptor. (Pseudo)polymorphism is common in both two- and three-dimensional crystals.[17] Metastable pseudopolymorphs were observed for both odd diesters; **ester-19** forms phases I and IV, and **ester-23** forms phases I, IV, and VIII. Phase I is the lowest energy form for both molecules. In this series of 1,3-disubstituted benzenes, there are two different causes of pseudopolymorphism: the kinetic formation of a metastable phase and induction by defects and edges. Although phase VIII is less dense than phase I, it is stabilized by weak hydrogen bonds and is therefore close in energy.[70] The competition between close packing and satisfaction of directional bonds provides multiple ways to achieve low potential energy structures, thereby leading to pseudopolymorphism. By contrast, phase IV is stabilized because of the reduction in interfacial energy it provides. Phase IV connects parallel yet offset domains of phase I, a lower energy configuration than mismatched phase I interfaces alone. The interfacial induction of (pseudo)polymorphs is particularly relevant to understanding nucleation of crystals from surfaces and nanoscale crystal growth. Concomitant pseudopolymorphs on a surface could induce concomitant polymorphism in three-dimensional molecular crystals[71] seeded from that surface.[72] The stabilization of interfaces by induction of different polymorphs is the basis of several methods of polymorph selection, including ledge-directed epitaxy, where steps of a single crystal promote growth of a given polymorph on the basis of its topographic coincidence with the step,[73,74] and polymer heteronucleation,[42] where different crystalline polymorphs are selected and discovered by growth from polymer surfaces.

Conclusions

Physisorbed monolayers at the liquid−solid interface are an effective model system for isolating and understanding the factors complicating three-dimensional crystallization, including the occurrence of more than one molecule in the asymmetric unit, structural changes associated with modification of functional groups, and polymorphism. The two-dimensional crystals of a series of 1,3-disubstituted benzenes are a particularly suitable example, exhibiting much of the complexity of three-dimensional crystals, but in a system where the effects of small molecular perturbations could be clearly identified. This series contains monolayers with unusually large Z' values for two- and three-dimensional crystals. These large Z' values were surprising in light of the fact that much simpler motifs ($Z' = 1$ or 0.5) are computed to be viable. Comparison of similar structures and pseudopolymorphs of the same compounds indicate that frustration between weak directional intermolecular interactions and close packing leads to these large Z' values. Even when the Z' values did not change, slight changes in molecular form induced dramatic changes in the two-dimensional packing. Identification of the structure-determining factors in this series was possible due to the reduction in dimensionality of the problem. It was found that an in-depth analysis of the possible packing motifs must take into account the preferred geometry of the isolated molecules, the density of possible phases, and electrostatic properties of the molecules. Applying this approach to the prediction of unknown two-dimensional

(68) Cyr, D. M.; Venkataraman, B.; Flynn, G. W.; Black, A.; Whitesides, G. M. *J. Phys. Chem.* **1996**, *100*, 13747−13759.
(69) Venkataraman, B.; Flynn, G. W.; Wilbur, J. L.; Folkers, J. P.; Whitesides, G. M. *J. Phys. Chem.* **1995**, *99*, 8684−8689.
(70) Among highly polymorphic organic compounds that have been structurally characterized, carbamazepine is the only one where the change between the four polymorphs is related primarily to weak hydrogen bonding. Grzesiak, A. L.; Lang, M.; Kim, K.; Matzger, A. J. *J. Pharm. Sci.* **2003**, *92*, 2260−2271.
(71) Bernstein, J.; Davey, R. J.; Henck, J. O. *Angew. Chem., Int. Ed.* **1999**, *38*, 3441−3461.
(72) For a novel mechanism of concomitant polymorphism in three-dimensions, see: Yu, L. *J. Am. Chem. Soc.* **2003**, *125*, 6380−6381.
(73) Bonafede, S. J.; Ward, M. D. *J. Am. Chem. Soc.* **1995**, *117*, 7853−7861.
(74) Carter, P. W.; Ward, M. D. *J. Am. Chem. Soc.* **1993**, *115*, 11521−11535.

structures will reveal if other factors must be considered as well. Illuminating these issues is critical to solving the closely analogous problem of predicting three-dimensional crystal structures.

Experimental Section

Scanning Tunneling Microscopy. A Nanoscope E STM (Digital Instruments) was used for all imaging. Highly oriented pyrolytic graphite (HOPG) (SPI-1 grade, Structure Probe Inc.) was used as a substrate for monolayer formation. A nearly saturated 1-phenyloctane solution of the desired molecule was made, and 1 μL was placed on freshly cleaved HOPG to obtain a self-assembled monolayer. The tips were made from Pt/Ir wire (20% Ir, 0.010 in. diameter, California Fine Wire) by mechanical cutting and shaped in situ by applying short voltage pulses. The quality of the tips was verified by scanning the HOPG surface under the monolayer at reduced bias voltage. All images are unfiltered. STM imaging was performed under ambient conditions, and typical STM settings include 300 pA of current and 600−1000 mV of bias voltage (sample positive). Measurements (Table 1) are checked against the graphite lattice and are the weighted averages of several imaging sessions whenever possible to minimize the effect of drift encountered in individual images.

Computational Modeling

Periodic and Cluster Calculations. The packing structures apparent from the metrics and symmetry of the STM images were modeled using Cerius[2] version 4.2 (Accelrys Inc.). Energy minimization was performed using a COMPASS force field.[75] The periodic three-dimensional models used in lattice energy calculations were minimized with a large *c*-axis, keeping out-of-plane parameters fixed. Nonperiodic assemblies from these models were overlaid on a fixed graphite slab for cluster simulations, from which the computed unit cell parameters (Table 1), models (Figures 2, 3, and 5), and densities[56] were obtained. The perturbation of the periodic structure upon simulation of adsorption to the graphite slab was minimal in all cases.

Individual Molecule Calculations. Equilibrium geometries, energies, and energy profiles with conformational changes were calculated on short-chain analogues of the molecules of interest using density functional theory (DFT) calculations at the B3LYP/6-31G** as implemented by Spartan '04 (Wavefunction Inc.).

Acknowledgment. This work was supported by start-up funds from the University of Michigan, a 3M Nontenured Faculty Grant, and the National Science Foundation (CHE-0316250). K.E.P. was a fellow of the NSF sponsored IGERT program for Molecularly Designed Electronic, Photonic, and Nanostructured Materials at the University of Michigan.

Supporting Information Available: Comparison of large-scale STM images of **ester-19** and **ester-20**; a table of densities and energies of **ester-19**, **ester-20**, **ester-22**, and **ester-23** in phases I and II; calculated energy profiles for torsional rotation and angles found in the CSD for alkane, ester, thioester, and ketone functionalities; large-scale STM image of **ester-23** showing dominance of phase I; STM image of **ester-23** showing the coincidence of phase IV formation with domain boundaries; thioester, ester, and ketone bond angles from the CSD; table showing the computed geometric differences between thioesters, esters, and ketones; high-resolution **ketone-19** (phase VI) STM image; model of **ketone-19** in phase VI showing hydrogen bonds; line scan from an STM image of **alkyne-18** in phase VII; filtered STM image of **alkyne-18** in phase VII; model of **ester-23** in phase VIII showing hydrogen bonds; synthesis and characterization of all compounds; experimental details of CSD searching. This material is available free of charge via the Internet at http:// pubs.acs.org.

JA0493446

(75) Sun, H. *J. Phys. Chem. B* **1998**, *102*, 7338−7364.